



Microaerobic Lifestyle at Nanomolar O₂ Concentrations Mediated by Low-Affinity Terminal Oxidases in Abundant Soil Bacteria

 Daniela Trojan,^a  Emilio Garcia-Robledo,^b  Dimitri V. Meier,^{a,*}  Bela Hausmann,^{a,c,d}  Niels Peter Revsbech,^e
 Stephanie A. Eichorst,^a  Dagmar Woebken^a

^aDivision of Microbial Ecology, Department of Microbiology and Ecosystem Science, Centre for Microbiology and Environmental Systems Science, University of Vienna, Vienna, Austria

^bDepartment of Biology, Faculty of Marine and Environmental Sciences, University of Cádiz, Cádiz, Spain

^cJoint Microbiome Facility of the Medical University of Vienna and the University of Vienna, Vienna, Austria

^dDepartment of Laboratory Medicine, Medical University of Vienna, Vienna, Austria

^eWATEC, Department of Biology, Aarhus University, Aarhus, Denmark

ABSTRACT High-affinity terminal oxidases (TOs) are believed to permit microbial respiration at low oxygen (O₂) levels. Genes encoding such oxidases are widespread, and their existence in microbial genomes is taken as an indicator for microaerobic respiration. We combined respiratory kinetics determined via highly sensitive optical trace O₂ sensors, genomics, and transcriptomics to test the hypothesis that high-affinity TOs are a prerequisite to respire micro- and nanooxic concentrations of O₂ in environmentally relevant model soil organisms: acidobacteria. Members of the *Acidobacteria* harbor branched respiratory chains terminating in low-affinity (*caa*₃-type cytochrome *c* oxidases) as well as high-affinity (*cbb*₃-type cytochrome *c* oxidases and/or *bd*-type quinol oxidases) TOs, potentially enabling them to cope with varying O₂ concentrations. The measured apparent *K_m* (*K_m(app)*) values for O₂ of selected strains ranged from 37 to 288 nmol O₂ liter⁻¹, comparable to values previously assigned to low-affinity TOs. Surprisingly, we could not detect the expression of the conventional high-affinity TO (*cbb*₃ type) at micro- and nanomolar O₂ concentrations but detected the expression of low-affinity TOs. To the best of our knowledge, this is the first observation of microaerobic respiration imparted by low-affinity TOs at O₂ concentrations as low as 1 nM. This challenges the standing hypothesis that a microaerobic lifestyle is exclusively imparted by the presence of high-affinity TOs. As low-affinity TOs are more efficient at generating ATP than high-affinity TOs, their utilization could provide a great benefit, even at low-nanomolar O₂ levels. Our findings highlight energy conservation strategies that could promote the success of *Acidobacteria* in soil but might also be important for as-yet-unrevealed microorganisms.

IMPORTANCE Low-oxygen habitats are widely distributed on Earth, ranging from the human intestine to soils. Microorganisms are assumed to have the capacity to respire low O₂ concentrations via high-affinity terminal oxidases. By utilizing strains of a ubiquitous and abundant group of soil bacteria, the *Acidobacteria*, and combining respiration kinetics, genomics, and transcriptomics, we provide evidence that these microorganisms use the energetically more efficient low-affinity terminal oxidases to respire low-nanomolar O₂ concentrations. This questions the standing hypothesis that the ability to respire traces of O₂ stems solely from the activity of high-affinity terminal oxidases. We propose that this energetically efficient strategy extends into other, so-far-unrevealed microbial clades. Our findings also demonstrate that physiological predictions regarding the utilization of different O₂ concentrations

Citation Trojan D, Garcia-Robledo E, Meier DV, Hausmann B, Revsbech NP, Eichorst SA, Woebken D. 2021. Microaerobic lifestyle at nanomolar O₂ concentrations mediated by low-affinity terminal oxidases in abundant soil bacteria. *mSystems* 6:e00250-21. <https://doi.org/10.1128/mSystems.00250-21>.

Editor Hans C. Bernstein, UiT—The Arctic University of Norway

Copyright © 2021 Trojan et al. This is an open-access article distributed under the terms of the [Creative Commons Attribution 4.0 International license](https://creativecommons.org/licenses/by/4.0/).

Address correspondence to Stephanie A. Eichorst, stephanie.eichorst@univie.ac.at.

* Present address: Dimitri V. Meier, Institute of Biogeochemistry and Pollutant Dynamics, Swiss Federal Institute of Technology, Zurich (ETH Zurich), Zurich, Switzerland.

Received 2 March 2021

Accepted 8 June 2021

Published 6 July 2021

based solely on the presence or absence of terminal oxidases in bacterial genomes can be misleading.

KEYWORDS terminal oxidase, oxygen, acidobacteria, kinetics, transcriptomics

Oxygen (O_2) has a high redox potential ($E_0' = +0.82$ V), which, together with its ubiquity, makes it a favorable electron acceptor for energy generation. The concentration of O_2 across numerous microbial habitats can vary from saturation to anoxia (1). It is believed that aerobic microorganisms meet these fluctuating conditions by harboring low- and high-affinity terminal oxidases (TOs), presumably allowing them to use a wide range of O_2 concentrations.

Terminal oxidases, which mediate the final redox reaction in the electron transport chain (ETC) during aerobic respiration, are grouped into three superfamilies: (i) heme-copper oxidases (HCOs), (ii) cytochrome *bd*-type oxidases, and (iii) alternative oxidases. HCOs are multisubunit complexes and function as cytochrome *c* or as quinol oxidases, contributing to energy conservation, the generation of a proton motive force, O_2 scavenging, and maintaining redox homeostasis (2, 3). Based on overall amino acid similarities of the catalytic subunits and differences of the proton channels, the HCO superfamily is classified into three families: A (subfamilies A1 and A2), B, and C (4). Family A oxidases have a low affinity for O_2 , with a reported Michaelis-Menten constant (K_m) for O_2 of 200 nmol O_2 liter⁻¹ (5). HCO families B and C are considered high-affinity TOs with high catalytic activity at low O_2 concentrations but reduced proton-pumping efficiency (6), with K_m values for the family C *cbb*₃-type oxidases of 7 to 40 nmol O_2 liter⁻¹ (7–9). The high-affinity cytochrome *bd*-type oxidase encoded by the *cydAB* genes (10–12) has reported K_m values of 3 to 8 nmol O_2 liter⁻¹ (13). Cytochrome *bd*-type oxidases do not pump protons across the membrane but contribute to proton motive force by using electrons from the extracytoplasmic side and protons from the cytoplasmic side (11).

High-affinity TOs are believed to sustain energy conservation at diminishing concentrations by enabling respiration at trace amounts of O_2 (i.e., micromolar O_2 concentrations) (14–16). Although there has been some suggestion that low-affinity TOs are present at micromolar O_2 concentrations in addition to high-affinity TOs (5), it remains unclear if the low-affinity TOs can actively and even solely contribute to respiration at these O_2 concentrations. At nanomolar O_2 concentrations, microorganisms transition from aerobic respiration to anaerobic-based metabolism (substrate-level phosphorylation or anaerobic respiration), referred to as the Pasteur point (17, 18). To the best of our knowledge, gene expression-based investigations of terminal oxidases at nanomolar O_2 concentrations are scarce (e.g., Gong et al. reported expression at O_2 levels of ≤ 200 nmol [19]), and therefore, it is mostly speculated that the high-affinity terminal oxidases are primarily responsible for energy production at low-nanomolar O_2 concentrations.

In soil, O_2 availability can be spatially and temporally dynamic, depending on the edaphic properties and microbial activity (20, 21). As such, microbial survival in soil is dependent on the ability to adapt to changes in local O_2 conditions. Environmental data and genome surveys suggest that both low- and high-affinity TOs are widely distributed in soils (16). *Acidobacteria* represent one of the most abundant and phylogenetically diverse phyla in soils worldwide (22–24) and are assigned a central role in carbon mineralization and plant polymeric carbon degradation (25, 26). Genes encoding high- and low-affinity TOs have been identified in several genomes of the phylum *Acidobacteria* (27), suggesting the capacity to respire across a wide gradient of O_2 concentrations. As respiratory flexibility can be attained through branched respiratory chains that terminate in multiple oxidases with different affinities for O_2 (15), this facet might be key to their ecological success in soil.

Using *Acidobacteria* as model soil organisms, we explored respiratory kinetics and evaluated their gene expression using whole-transcriptome sequencing and reverse transcription-quantitative PCR (RT-qPCR) across decreasing low-micromolar to nanomolar O_2 concentrations. As such, we could test the hypothesis that at micro- to

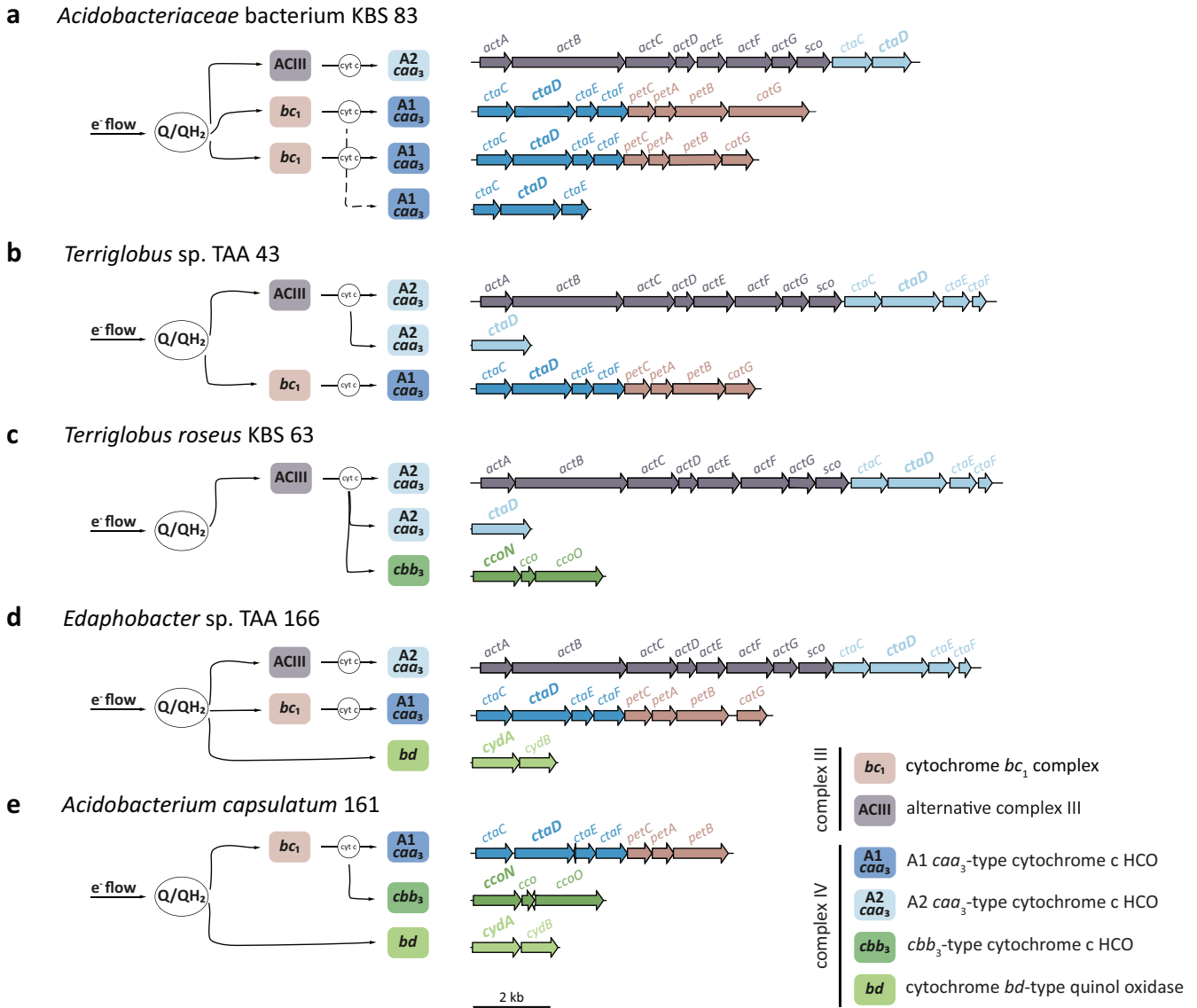


FIG 1 Schematic representation of electron (e^-) flow in the predicted branched electron transport chains among the acidobacterial strains and organization of the respiratory genes in the respective genomes. The low- and high-affinity terminal oxidases of complex IV are depicted in blue and green, respectively. Complex III is depicted in gray (alternative complex III [ACIII]) or brown (cytochrome bc_1 complex [bc_1]). The quinone/quinol pools and cytochrome c are depicted as Q/QH₂ and cyt c , respectively. The catalytic subunits of terminal oxidases are in boldface type. The dashed line in panel a indicates the electron flow via two possible bc_1 complexes. Locus tags of the genes are listed in Data Set S1 in the supplemental material.

nanomolar O₂ concentrations, aerobic respiration is mediated by high-affinity TOs. Our data demonstrate that O₂ concentrations down to the nanomolar level can be respired by low-affinity TOs, an unexpected physiological response, suggesting that the ability to respire O₂ under micro- to nanooxic conditions is not exclusively based on the presence and activity of high-affinity TOs.

RESULTS

Distribution of low- and high-affinity terminal oxidases. Five acidobacterial strains were chosen to explore their respiratory kinetics, and of these strains, three were chosen to explore their TO expression patterns across nanomolar O₂ concentrations. All strains harbored branched respiratory chains terminating in multiple oxidases (Fig. 1; see also Data Set S1 in the supplemental material). They differed in their distributions of low- and high-affinity TOs (complex IV) as well as of complexes III (cytochrome bc_1 complex and/or alternative complex III [ACIII]) (Fig. 1; Data Set S1).

Acidobacteriaceae bacterium KBS 83 and *Terriglobus* sp. strain TAA 43 harbored multiple homologs of only low-affinity TOs; *Acidobacteriaceae* bacterium KBS 83 encoded three A1 *caa*₃ HCOs and one A2 *caa*₃ HCO (Fig. 1a), whereas *Terriglobus* sp. TAA 43 had one A1 *caa*₃ HCO and two A2 *caa*₃ HCOs encoded (Fig. 1b). *Terriglobus roseus* KBS 63 had two homologs of A2 *caa*₃ HCOs (Fig. 1c), *Edaphobacter* sp. strain TAA 166 had one A1 *caa*₃ HCO and one A2 *caa*₃ HCO (Fig. 1d), and *Acidobacterium capsulatum* 161 had one A1 *caa*₃ HCO encoded (Fig. 1e). In addition to low-affinity TOs, *T. roseus* KBS 63, *Edaphobacter* sp. TAA 166, and *A. capsulatum* 161 also harbored high-affinity TOs: *T. roseus* KBS 63 had a *cbb*₃ type (C HCO) (Fig. 1c), *Edaphobacter* sp. TAA 166 had a *bd* type (Fig. 1d), and *A. capsulatum* 161 had both types (Fig. 1e).

There was consistent gene synteny for the A1 *caa*₃ HCO, A2 *caa*₃ HCO, C *cbb*₃ HCO, and *bd*-type quinol oxidases and the adjacent complex III genes among the acidobacterial strains (Fig. 1). Genes for the A1 *caa*₃ HCO were always located in an operon upstream of the genes encoding the *bc*₁ complex (described here as a “superoperon”) (Fig. 1). The A2 *caa*₃ HCO also occurred in a superoperon with the genes encoding ACIII, instead of the *bc*₁ complex, and were located downstream of the ACIII genes (Fig. 1). Additional, single homologs of either the A1 or A2 *caa*₃-type oxidases were detected in the genomes of *Acidobacteriaceae* bacterium KBS 83 (Fig. 1a), *Terriglobus* sp. TAA 43 (Fig. 1b), and *T. roseus* KBS 63 (Fig. 1c). *T. roseus* KBS 63 (Fig. 1c) and *A. capsulatum* 161 (Fig. 1e) contained *cbb*₃ operons consisting of genes for *cbb*₃ subunits N and O as well as an additional *cco* gene of unknown function. *Edaphobacter* sp. TAA 166 (Fig. 1d) and *A. capsulatum* 161 (Fig. 1e) contained both *cydA* and *cydB* subunits for the *bd*-type quinol oxidase.

Assessment of O₂ respiratory kinetics. We determined the O₂ respiration rates and population apparent K_m ($K_{m(\text{app})}$) values for the five acidobacterial strains with differing distributions of high- and low-affinity TOs in exponential phase (non-energy limited) with only O₂-limiting respiration rates (Fig. 2). All strains followed Michaelis-Menten-type kinetics. *Acidobacteriaceae* bacterium KBS 83 and *Terriglobus* sp. TAA 43, both harboring only low-affinity TOs, had $K_{m(\text{app})}$ values for O₂ of 166 ± 11 nmol O₂ liter⁻¹ (Fig. 2a) and 250 ± 5 nmol O₂ liter⁻¹ (Fig. 2d), respectively. The maximum population respiration rate (V_{max}) of *Acidobacteriaceae* bacterium KBS 83 was on average 355 ± 12 nmol O₂ liter⁻¹ h⁻¹, and the maximum respiration rates per cell (R_{max}) progressively decreased over time from 9.8 to 6.8 ± 0.4 fmol O₂ cell⁻¹ h⁻¹ (Fig. 2a; Table S1). The V_{max} of *Terriglobus* sp. TAA 43 was 998 ± 6 nmol O₂ liter⁻¹ h⁻¹, and the R_{max} was constant at 2.6 ± 0.02 fmol O₂ cell⁻¹ h⁻¹ (Fig. 2d).

For *T. roseus* KBS 63 and *Edaphobacter* sp. TAA 166, harboring both low- and either a *cbb*₃- or *bd*-type high-affinity TO, the $K_{m(\text{app})}$ values were 113 ± 24 nmol O₂ liter⁻¹ and 288 ± 34 nmol O₂ liter⁻¹, respectively (Fig. 2b and e). The V_{max} values of *T. roseus* KBS 63 and *Edaphobacter* sp. TAA 166 (201 ± 35 and 604 ± 69 nmol O₂ liter⁻¹ h⁻¹, respectively) as well as their R_{max} values (0.38 ± 0.07 fmol O₂ cell⁻¹ h⁻¹ and 0.16 ± 0.02 fmol O₂ cell⁻¹ h⁻¹, respectively) were stable throughout the incubations (Fig. 2b and e). The $K_{m(\text{app})}$ value for *A. capsulatum* 161, harboring one low-affinity and both types of high-affinity TOs, decreased from 99 ± 14 to 37 ± 2 nmol O₂ liter⁻¹ (Table S2), with a final $K_{m(\text{app})}$ value 1 order of magnitude lower than the values of the other investigated strains (Fig. 2c). In addition, the V_{max} and R_{max} of *A. capsulatum* 161 progressively increased during the whole period of measurements from $2,150 \pm 156$ to $3,609 \pm 430$ nmol O₂ liter⁻¹ h⁻¹ (Table S2) and from 0.17 ± 0.01 to 0.26 ± 0.03 fmol O₂ cell⁻¹ h⁻¹, respectively (Fig. 2c). The respiration rates rose to a maximum as O₂ concentrations increased and then descended to a nonzero asymptote. Additionally, the velocity curves saturated rapidly, compared to the other strains (Fig. 2e).

Differential gene expression due to changing O₂ concentrations. Of the five strains, we selected three that encompass different combinations of low- and high-affinity TOs to compare changes in gene expression levels when exposed to different, decreasing O₂ concentrations. Transcriptome analysis of *Acidobacteriaceae* bacterium KBS 83, *T. roseus* KBS 63, and *A. capsulatum* 161 showed that in the course of the time series, 5,121 (93% of all annotated genes), 4,239 (97%), and 3,321 (97%) genes,

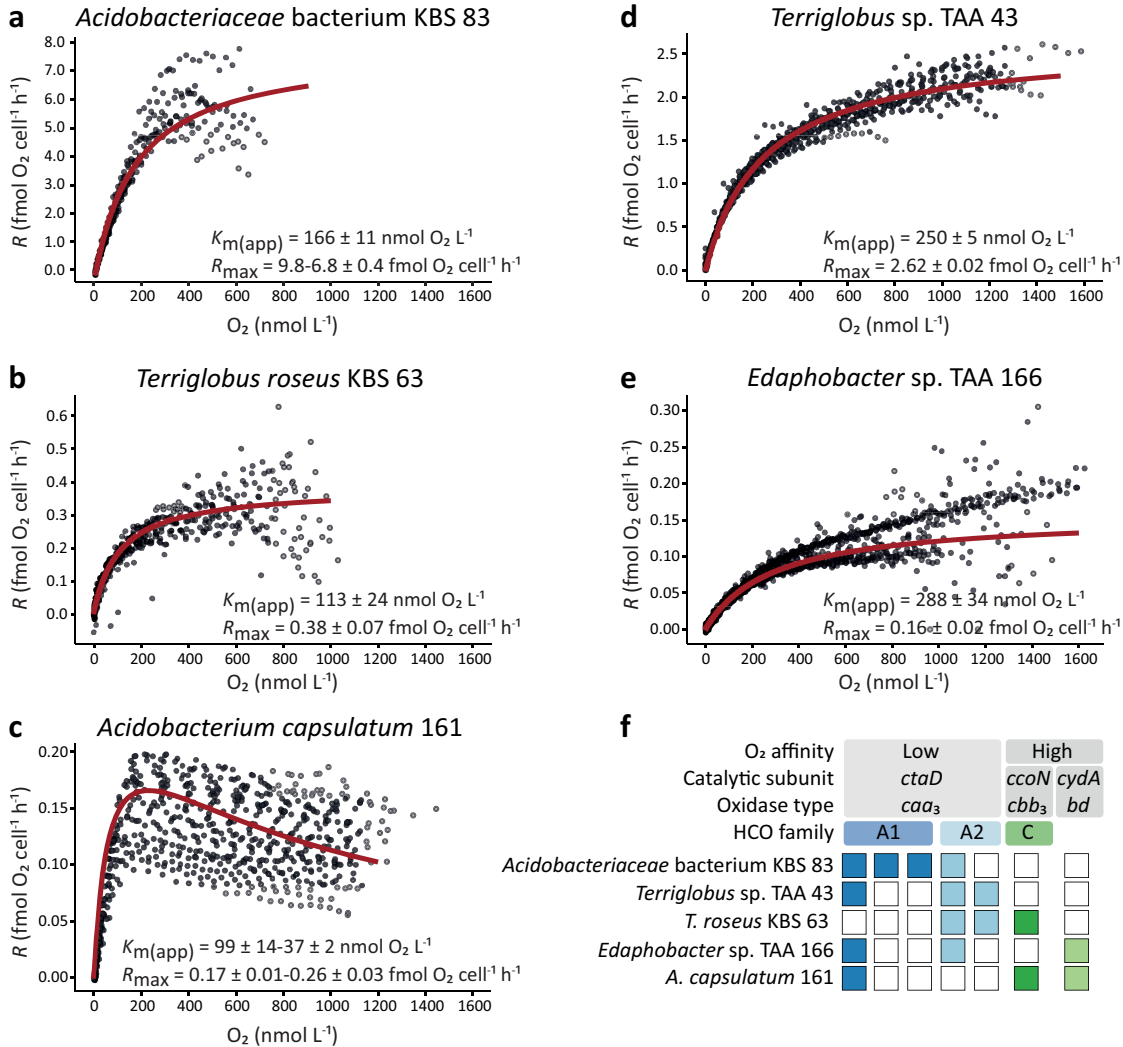


FIG 2 (a to e) Population respiratory kinetics of *Acidobacteriaceae* bacterium KBS 83 (a), *T. roseus* KBS 63 (b), *A. capsulatum* 161 (c), *Terriglobus* sp. TAA 43 (d), and *Edaphobacter* sp. TAA 166 (e). (f) Overview of the genomic identification of genes encoding terminal oxidases across the five acidobacterial strains. In panels a to e, the red curves indicate the Michaelis-Menten model best fit of the data. Across all strains, gray circles depict average respiration rates for biological triplicates over time, except for (i) *Acidobacteriaceae* bacterium KBS 83, where the gray circles represent the average respiration rates from biological duplicates, and (ii) *A. capsulatum* 161, where the individual replicates are depicted to illustrate the increase in respiration rates during the 24-h incubation period. See Tables S1 and S2 in the supplemental material for additional results of the temporal changes of kinetic parameters of *Acidobacteriaceae* bacterium KBS 83 and *A. capsulatum* 161, respectively. Apparent half-saturation constants ($K_{m(app)}$) and maximum respiration rates (R_{max}) are means \pm standard errors.

respectively, were transcribed at least at one time point across the O_2 concentrations (Table S5).

The decrease from 10 to $0.1 \mu\text{mol O}_2 \text{ liter}^{-1}$ had the greatest impact on the transcriptomes of all three strains, with the highest number of significantly differentially expressed genes observed (Fig. 3a). Among 1,602 (31%) differentially expressed genes of *Acidobacteriaceae* bacterium KBS 83, 16% were upregulated and 15% were downregulated upon the transition from 10 to $0.1 \mu\text{mol O}_2 \text{ liter}^{-1}$ after cells equilibrated for 60 min at each respective O_2 concentration (Fig. 3b). For *T. roseus* KBS 63 and *A. capsulatum* 161, 38% (20% upregulated and 18% downregulated) and 81% (41% upregulated and 40% downregulated), respectively, were differentially expressed upon this transition from 10 to $0.1 \mu\text{mol O}_2 \text{ liter}^{-1}$ (Fig. 3b). Comparatively, there were few to no significant expression changes when transitioning from 0.1 to $0.001 \mu\text{mol O}_2 \text{ liter}^{-1}$ regardless of the equilibration time at the lower O_2 concentration; similar patterns were

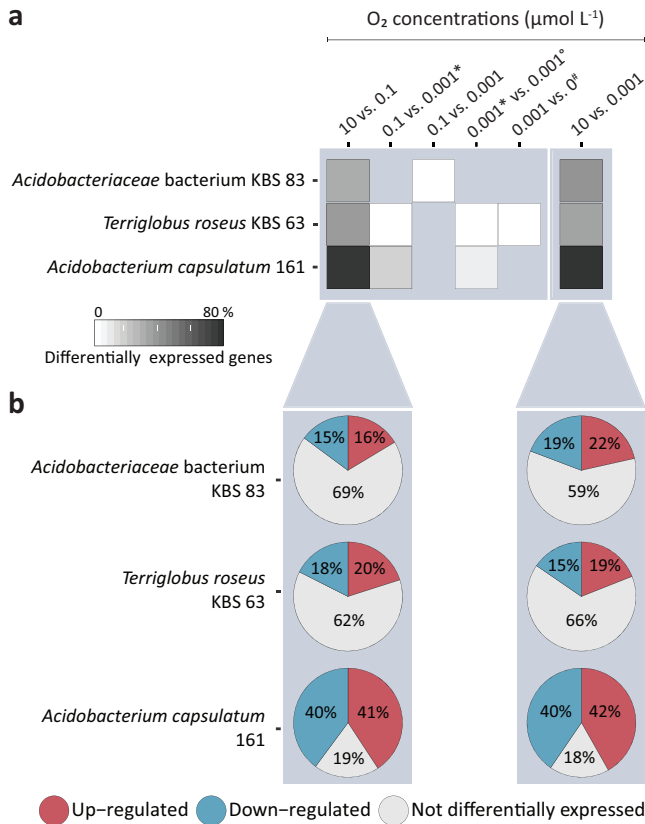


FIG 3 Impact of decreasing O₂ concentrations on the transcriptomes of *Acidobacteriaceae* bacterium KBS 83, *T. roseus* KBS 63, and *A. capsulatum* 161. (a) Heat map depicting the proportions of genes that were differentially expressed ($P < 0.05$) between two O₂ concentrations (micromoles of O₂ per liter). The darker the color, the higher the proportion of genes whose expression has significantly changed between two O₂ concentrations. All comparisons were done after 60 min at each respective O₂ concentration, with three exceptions: * depicts differential expression after 10 min, # depicts differential expression after 15 min, and ° depicts differential expression after 50 min. A concentration of 0.001 μmol O₂ liter⁻¹ is defined as apparent anoxia: O₂ was still supplied (3.8 to 10.1 μmol O₂ min⁻¹) but could no longer be accurately determined. A concentration of 0 μmol O₂ liter⁻¹ indicates no O₂ supply. (b) Breakdown of differentially expressed genes ($P < 0.05$) for 10 versus 0.1 μmol O₂ liter⁻¹ and 10 versus 0.001 μmol O₂ liter⁻¹.

observed in the transcriptome of *T. roseus* KBS 63 when transitioning from 0.001 to 0 μmol O₂ liter⁻¹ (Fig. 3a). The comparison between 10 and 0.001 μmol O₂ liter⁻¹ revealed the same overall transcription pattern as that for the transition from 10 to 0.1 μmol O₂ liter⁻¹ (Fig. 3). During these incubations, O₂ was decreased in a stepwise manner from 10 μmol O₂ liter⁻¹ to anoxic conditions (<0.0005 μmol O₂ liter⁻¹) (Fig. 4). Below 0.01 μmol O₂ liter⁻¹, *Acidobacteriaceae* bacterium KBS 83, harboring only low-affinity TOs, consumed O₂ at a respiration rate lower than the rate at which O₂ was supplied, causing concentrations to never drop to anoxic conditions (Fig. 4a).

In contrast, strains harboring both low- and high-affinity TOs (*T. roseus* KBS 63 and *A. capsulatum* 161) consumed all the supplied O₂ at our lowest provided rate (i.e., 5.1 μmol O₂ min⁻¹ [*T. roseus* KBS 63] and 10.1 μmol O₂ min⁻¹ [*A. capsulatum* 161]). Their O₂ uptake rates were higher than the O₂ inflow rate, thereby creating an apparent anoxic environment below our detection limit of 0.0005 μmol O₂ liter⁻¹ (Fig. 4c and e).

Transcriptional responses of branching electron transport chain key genes and terminal oxidases to decreasing O₂ concentrations. We further explored the transcriptional changes of TOs (complexes III and IV) of the ETC by focusing on key functional genes of these complexes (Fig. 4; Data Set S2).

(i) *Acidobacteriaceae* bacterium KBS 83. Continuous expression of two out of the four low-affinity *caa*₃-type cytochrome *c* oxidases, one of the *bc*₁-A1 *caa*₃ superoperons

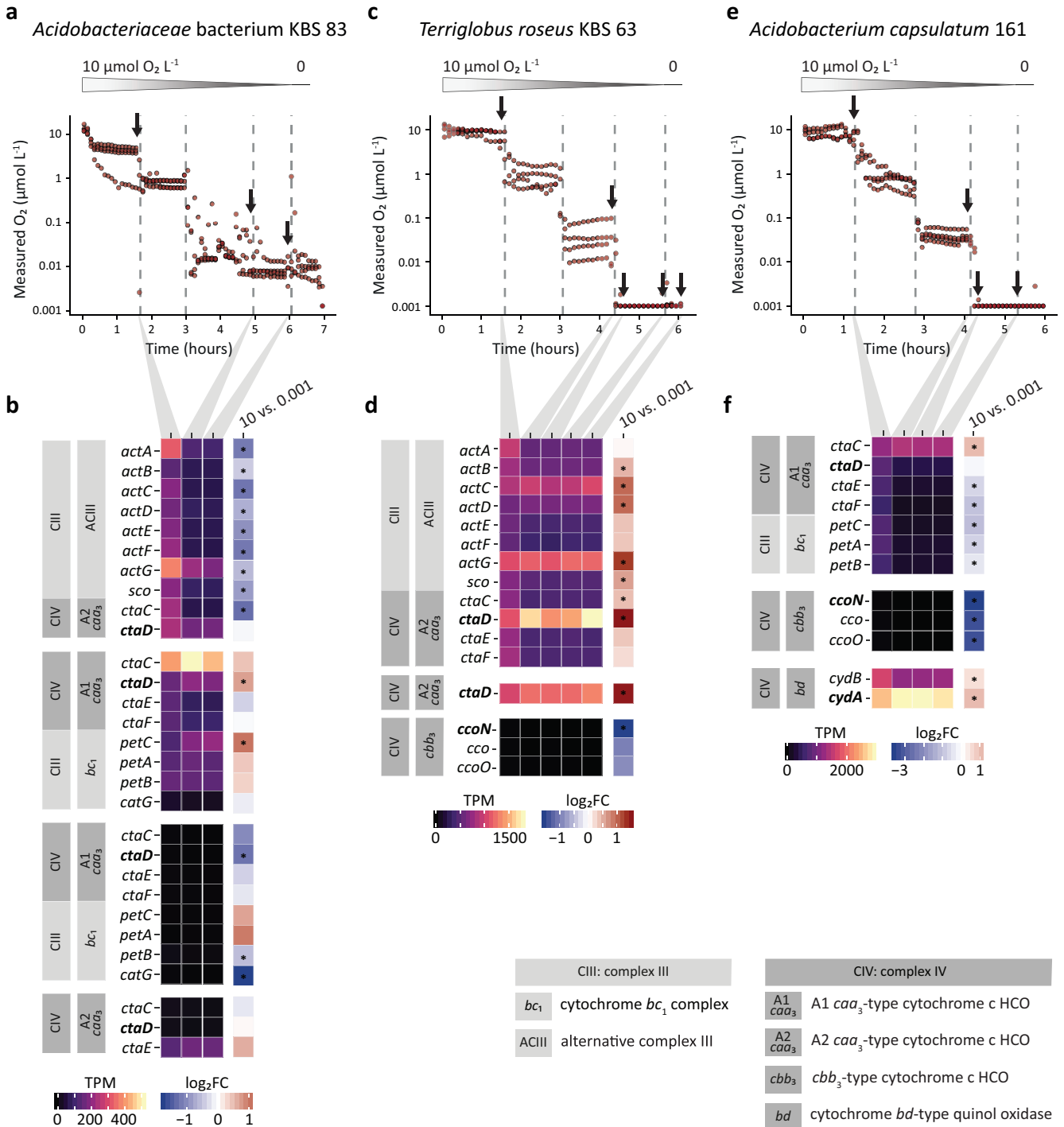


FIG 4 Respiration dynamics and transcription patterns of complex III and IV genes in the electron transport chain of *Acidobacteriaceae* bacterium KBS 83, *T. roseus* KBS 63, and *A. capsulatum* 161 exposed to decreasing O₂ concentrations. (a, c, and e) Measured O₂ concentrations in cultures of the three strains over time (*n* = 4 biological replicates/strain) during O₂-limited incubations. O₂ was decreased in a stepwise manner from 10 to 1 to 0.1 to 0.001 to 0 μmol O₂ liter⁻¹. Vertical dashed lines depict the transition time points, while arrows indicate transcriptome sampling points after 60, 10, or 15 min at the respective O₂ concentrations. (b, d, and f) Time-resolved gene expression of complex III and complex IV at 10, 0.1, 0.001, and 0 μmol O₂ liter⁻¹. Heat maps show average transcript per million (TPM) values from biological replicates (*n* = 3). The last column depicts log₂ fold changes (log₂FC) of transcripts between 10 and 0.001 μmol O₂ liter⁻¹ after 60 min at the respective O₂ concentrations. Downregulation is depicted in blue, and upregulation is in red. Asterisks depict significant differential expression (*P* < 0.05). Catalytic subunits of terminal oxidases are in boldface type. A concentration of 0.001 μmol O₂ liter⁻¹ is defined as apparent anoxia: O₂ was still supplied (3.8 to 10.1 μmol O₂ min⁻¹) but could no longer be accurately determined. A concentration of 0 μmol O₂ liter⁻¹ indicates no O₂ supply. Data for all replicates, gene locus tags, and further details are listed in Data Set S2 in the supplemental material.

and the ACIII-A2 *caa*₃ superoperon, was observed across all investigated O₂ concentrations, even after exposure to 0.001 μmol O₂ liter⁻¹ for an extended period of time (Fig. 4b; Data Set S2); similar patterns were observed by RT-qPCR (Fig. S1a). All genes of superoperon ACIII-A2 *caa*₃ exhibited significantly lower expression levels at 0.001 than at 10 μmol O₂ liter⁻¹ ($P < 0.05$), yet the catalytic subunit *ctaD* of the A2 HCO was consistently highly expressed across O₂ concentrations and not significantly downregulated (Fig. 4b). In contrast, *ctaD* of the A1 HCO complex together with *petC* of the *bc*₁ complex were significantly upregulated at 0.001 μmol O₂ liter⁻¹ ($P < 0.05$). The transcription level of the electron-receiving subunit II (*ctaC*) was higher than that of the rest of the *bc*₁-A1 *caa*₃ superoperon and remained high upon transitions to lower O₂ concentrations (Fig. 4b); the same responses were observed within the first 10 min after shifts of oxygenation by RT-qPCR (Fig. S1a). We still observed gene expression 15 min after the O₂ supply was ceased (Fig. S1a). Even then, the O₂ concentration did not fall below 0.01 μmol O₂ liter⁻¹ (Fig. 4a), and *Acidobacteriaceae* bacterium KBS 83 was still expressing its TOs after 3 h at 0.01 μmol O₂ liter⁻¹ (Fig. 4b). Of the other complexes IV, only *ctaE* that encodes subunit III of the single complex IV exhibited high expression levels (Fig. 4b).

(ii) *T. roseus* KBS 63. The expression levels (transcripts per million [TPM]) of the catalytic subunit of the *ccb*₃-type high-affinity TO (*ccoN*) across the investigated O₂ concentrations were low (Fig. 4d; Data Set 2) and too low for reliable quantification by RT-qPCR (Fig. S1b). The catalytic subunits of both low-affinity A2 HCO TOs (*ctaD*) exhibited the highest expression levels and were transcribed at significantly higher levels ($P < 0.0001$) at 0.001 than at 10 μmol O₂ liter⁻¹ (Fig. 4d). All other genes of the ACIII-A2 *caa*₃ superoperon were also upregulated (Fig. 4b). After a shift to anoxic conditions, the single *ctaD* gene was still expressed and upregulated (Fig. S1b).

(iii) *A. capsulatum* 161. The *ccb*₃-type high-affinity TO was transcribed at low levels at 10 μmol O₂ liter⁻¹ and was significantly downregulated ($P < 0.0001$) at all subsequent lower concentrations (down to 0.001 μmol O₂ liter⁻¹) (Fig. 4f; Data Set S2). Expression of the *ccb*₃-type high-affinity TO by RT-qPCR was seen from 10 to 0.1 μmol O₂ but only for 10 min at this concentration as measured by RT-qPCR (Fig. S1c). In contrast, the *bd*-type TO (*cydAB*) was expressed at all investigated O₂ concentrations (10 to 0.001 μmol O₂ liter⁻¹). The relative abundance of *cydA* transcripts was very high under all O₂ tensions (58-fold higher than that of the *rpoB* gene) (Data Set S2). RT-qPCR showed a clear and significant ($P \leq 0.05$) upregulation of the catalytic subunit *cydA* (Fig. S1c). Furthermore, *cydA* transcription levels were always high, even under anoxic conditions. The *ctaD* gene, encoding the catalytic subunit of the low-affinity A1 HCO, was continuously transcribed across all O₂ concentrations as detected by transcriptomics and RT-qPCR (Fig. 4f; Fig. S1c). However, the proportion of *ctaD* transcripts decreased under anoxic conditions (Fig. 4f).

DISCUSSION

Members of an abundant soil phylum, the *Acidobacteria*, respire environmentally relevant micro- and nanomolar O₂ concentrations with the use of low-affinity TOs. Respiratory kinetics were determined using highly sensitive optical sensors, which allowed us to study the O₂ kinetics with a high degree of accuracy. Our findings extend the current knowledge on O₂ kinetics to species outside the *Proteobacteria*.

Acidobacteria harbor branched respiratory chains terminating in multiple complexes IV with either low or high affinities for O₂. Branched ETCs terminating in differing terminal electron acceptors (such as O₂, NO₃, or NO₂) are typically found in bacteria, providing flexibility when exposed to various environmental conditions (14, 15). Enzymatic redundancy in using a single electron acceptor (such as O₂) can provide additional flexibility due to varying substrate affinities, allowing the microorganism to respire most efficiently across different concentrations, as seen in organisms living at the oxic-anoxic interface (28–34). This flexibility extends to our investigated soil acidobacterial strains, as many of them have branched ETCs that terminate in multiple complexes IV with either low or high affinities for O₂ (Fig. 1). Furthermore, in select strains,

genes for complex IV were detected in superoperons together with genes for complex III, either bc_1 or alternative complexes III (Fig. 1), as previously seen in other members of the *Acidobacteria* and further phyla (35, 36), potentially functioning as respiratory supercomplexes (37–39). Although the physiological relevance of supercomplexes is still unclear (40), we suggest that this physical association might provide additional metabolic flexibility in the acidobacteria. The close association could allow a more favorable transfer between complexes, bypassing soluble electron carriers (39). Nevertheless, follow-up investigations will be needed to elucidate the advantage of the supercomplexes. The complex IV genes were also found independent from complex III genes in three strains (Fig. 1).

The conventional high-affinity cbb_3 -type TO does not actively contribute to the capacity to respire O_2 at nanomolar concentrations. High-affinity TOs are historically believed to enable respiration and provide the capacity for energy conservation at trace concentrations of O_2 , a physiology that was shown to be widespread among bacteria and archaea of diverse environments, as suggested by genome surveys (16). Yet in the investigated acidobacterial strains, the cbb_3 -type high-affinity TO did not impart the capacity to respire O_2 at nanomolar concentrations. In our experimental setup, strains harboring high-affinity TO genes had the potential to develop low apparent K_m values by expressing these TO genes under O_2 -limited conditions, as in our incubations, the cells were exposed to multiple oxic-to-anoxic gradients over a 24-h period. Furthermore, our investigated strains harbor the minimal core, the CcoNO protein dyad (41), for the functionality of the enzyme (Fig. 1). Expression of the cbb_3 -type oxidase could not be detected below $10 \mu\text{mol } O_2 \text{ liter}^{-1}$ in both strains *T. roseus* KBS 63 and *A. capsulatum* 161 (Fig. 4), although they indeed consumed O_2 down to (apparent) anoxia. Compared to reported $K_{m(\text{app})}$ values for O_2 of *Proteobacteria* strains harboring cbb_3 -type oxidases measured by the same method (42), the $K_{m(\text{app})}$ value of *T. roseus* KBS 63 was high ($113 \text{ nmol } O_2 \text{ liter}^{-1}$) (Fig. 2b). This further provides evidence for the activity of the low-affinity oxidase(s) and suggests that it might be used for respiration in environments with low O_2 concentrations, such as the heterogeneous soil environment. O_2 fluctuations in soil are dynamic, and exposure to low-nanomolar O_2 concentrations might be temporally limited to short intervals (43). Therefore, we hypothesize that the investment in the expression of a less-energy-efficient TO (the high-affinity cbb_3 type) (44, 45) will not provide any competitive advantage for these investigated time intervals. At this time, it is unclear if the cbb_3 -type oxidase has lost its function to generate proton motive force in these strains. Alternatively, cbb_3 TO expression in *T. roseus* KBS 63 and *A. capsulatum* 161 could be triggered by other factors, such as nutrient limitation or carbon depletion, as recently reported for *Shewanella oneidensis* (46).

Utilization of acidobacterial bd -type oxidases at nanomolar O_2 concentrations. The bd -type oxidases are another type of high-affinity TO, which are less efficient at creating the charge gradient for ATP generation as they do not pump protons across the membrane but generate a proton motive force by transmembrane charge separation (12). Expression data showed a clear and significant upregulation of the catalytic subunit *cydA* gene as O_2 concentrations decreased in *A. capsulatum* 161 (Fig. 4f; see also Fig. S1c in the supplemental material). This suggests that the bd -type oxidase contributed to the respiratory activity under trace O_2 conditions. In contrast, the cbb_3 type was transcribed only at low levels at $10 \mu\text{mol } O_2 \text{ liter}^{-1}$ and was significantly downregulated ($P < 0.0001$) at all subsequent lower concentrations (Fig. 4f; Fig. S1c). However, the use of the bd -type oxidase for respiration activity appears to be strain dependent. In another strain harboring a high-affinity bd -type oxidase (*Edaphobacter* sp. TAA 166), the expression of *cydA* could not be detected at any examined O_2 concentration; rather, the low-affinity TOs were expressed across these O_2 concentrations (RT-qPCR data not shown). Here, the bd -type oxidase could be contributing to physiological functions other than respiratory O_2 reductions, such as reactive oxygen species (ROS) stress, iron deficiency, or nitric oxide stress responses (11, 12, 47).

Although the bd -type oxidases are not as efficient at creating a charge gradient, these oxidases have functional and structural characteristics that favor a faster electron

flux than *cbb*₃-type oxidases (11, 12), which could be advantageous under conditions with plentiful reducing potential stemming from carbon surplus. For instance, they receive electrons directly from the quinol pool and thereby take a shortcut through the branched ETC, bypassing any complexes III (Fig. 1). In support of this conjecture, *bd*-type oxidase genes were found to be more prevalent in environments where carbon is in excess, such as host-associated environments and carbon-rich forest soils compared to carbon-poor agricultural soils (16). As our investigated conditions were a combination of carbon surplus and O₂ limitation, we therefore hypothesize that this selected for the utilization of the *bd*-type oxidase compared to the *cbb*₃ type in *A. capsulatum* 161.

The strain expressing the *bd*-type oxidase under low O₂ concentrations (*A. capsulatum* 161) was the only one that was inhibited by high O₂ concentrations at its maximum respiration rate (R_{\max}) (Fig. 2c) (>250 nmol O₂ liter⁻¹). Furthermore, its $K_{m(\text{app})}$ value decreased over multiple oxic-anoxic shifts ($n = 17$) within 24 h, indicating a need for less substrate and, therefore, an adaptation to these conditions. This temporal kinetic development was previously observed for marine *Proteobacteria* (42). The final estimated $K_{m(\text{app})}$ value of *A. capsulatum* 161 (37 nmol O₂ liter⁻¹) suggests a mixed activity of low- and high-affinity TOs (Fig. 2c), with its high-affinity TO contributing a large portion of the $K_{m(\text{app})}$ value. This respiratory kinetic activity of *A. capsulatum* 161 suggests that this strain can use different O₂ concentrations due to its enzymes' O₂ affinities. Presumably, this strain has a different strategy to exploit microoxic niches compared to the other investigated strains, which also could be advantageous in the soil when exposed to spatiotemporal gradients and diffusion limitations.

Acidobacterial low-affinity TOs are used at nanomolar O₂ concentrations.

Acidobacterial low-affinity *caa*₃-type HCOs are functioning at previously unknown nanomolar O₂ concentrations, as shown in the investigated strains (Fig. 4; Fig. S1). The use of low-affinity A HCOs at low concentrations of O₂ is energetically favorable, as they have more free energy available for driving proton translocation due to poor O₂ binding (44, 45) and a more efficient, and thus favorable, gating for proton leakage (44) than high-affinity TOs. High-affinity C HCOs typically exhibit higher catalytic activity at lower O₂ concentrations due to a different redox-driven proton-pumping mechanism that allows an increased electron transfer rate and a faster reduction of O₂ (48). Still, these high affinities come with a reduced proton-pumping efficiency (6, 44).

Many of the genes for the A2 *caa*₃ HCO in *T. roseus* KBS 63 were not only expressed across varying O₂ concentrations but in some cases also even upregulated at lower O₂ concentrations (Fig. 4d; Fig. S1b). A continuous expression of low-affinity *caa*₃-type TOs at low O₂ concentrations was previously reported in aerobic marine bacterial species (19, 49); however, in that study (19), the high-affinity *cbb*₃-type TO was upregulated at <0.2 μmol O₂ liter⁻¹. In our study, we did not observe any measurable contribution via transcriptomics or qPCR of the high-affinity *cbb*₃-type TO in any of the strains at 10 to 0.001 μmol O₂ liter⁻¹, although we cannot completely rule out the possibility of a minor contribution (undetectable with our current methods) of the *cbb*₃-type TO. Likewise, it is conceivable that high-affinity *cbb*₃-type TOs function only at extremely low concentrations of O₂ (<1 nmol O₂ liter⁻¹), which we currently cannot establish, maintain, and measure in the laboratory. Nevertheless, it appears that at the low O₂ concentrations (down to 1 nmol O₂ liter⁻¹) investigated in this study, *T. roseus* KBS 63 definitely prioritizes the low-affinity TOs. The energetic advantage of the low-affinity TOs might explain the strategy of *T. roseus* KBS 63 to invest in the high expression and upregulation of A2 *caa*₃ HCOs, compared to its *cbb*₃-type high-affinity TO (Fig. 4d; Fig. S1b).

In contrast, *Acidobacteriaceae* bacterium KBS 83 harbored only low-affinity TOs (*caa*₃ type) and was able to respire at O₂ concentrations of 10 μmol O₂ liter⁻¹ and lower. Below 0.01 μmol O₂ liter⁻¹, it consumed O₂ at a respiration rate lower than the rate at which O₂ was supplied, causing concentrations not to reach anoxic conditions (Fig. 4a). However, complete consumption to anoxia was reached during the kinetics

measurement experiments, reflecting the capacity to respire O_2 at trace concentrations. This difference could be explained by a lower cell density in the incubations for transcriptome analysis, not allowing these incubations to reach anoxia during the time course of the incubations simply due to cell number. Alternatively, O_2 diffusion could explain this discrepancy; this is unlikely as it was not observed in other incubations of the investigated acidobacteria. Efficient energy conservation (generating more ATP/electron) would be a vital survival strategy in times of substrate limitation in environments such as soil. It therefore might be an advantage to use low-affinity TOs even at nanomolar O_2 concentrations as they, despite their lower reaction rate, ultimately drive more charges across the membrane per mole of O_2 , making them more efficient in energy conservation.

It appears that the capacity of *Acidobacteriaceae* bacterium KBS 83 to respire O_2 under low concentrations was limited, as seen by the decreasing V_{max} and R_{max} over time (Table S1). Its $K_{m(app)}$ value (166 nmol O_2 liter $^{-1}$) is lower than and in contrast to the previously reported K_m value for the *caa* $_3$ -type oxidase of *Pseudomonas aeruginosa* (4,300 nmol O_2 liter $^{-1}$) (8) but in the same range as the one for the low-affinity cytochrome *bo* $_3$ ubiquinol oxidase of *Escherichia coli* (200 nmol O_2 liter $^{-1}$) (5). Although it is difficult to compare K_m values across studies as the determined K_m values can differ dramatically depending on the applied approach (8, 50), we want to stress the fact that one has to be careful with historically set benchmarks that propagate in the literature. The determined $K_{m(app)}$ values of our study represent ecophysiological relevant estimates as we used whole populations and intact cells as well as highly sensitive optical sensors with an extremely low detection limit.

Conclusion. Microorganisms frequently have to cope with changing O_2 tensions; therefore, having the flexibility to use a wide range of O_2 concentrations is beneficial (16). Here, we show that members of a dominant and ubiquitous soil phylum (22, 24, 26), the *Acidobacteria*, have branched ETCs that terminate in multiple oxidases (high- and low-affinity TOs), providing them with respiratory flexibility and adaptability to environmental changes (14–16). More specifically, their low-affinity TOs are functioning at nanomolar O_2 concentrations, presumably providing a great benefit for soil acidobacteria as they are more efficient in generating ATP than high-affinity TOs (44). We hypothesize that this strategy could be employed by other bacterial clades in soil as well as other habitats. Follow-up work is needed to ascertain if respiration at nanomolar O_2 concentrations allows biomass production or population growth in the long run during exposure to such low O_2 levels. In addition, low O_2 concentrations and nutrient-rich conditions selected for the expression of the high-affinity *bd*-type oxidase rather than the *cbb* $_3$ type, which presumably provides a more optimal balance of substrate oxidation and ATP production under these conditions. Follow-up studies are needed to elucidate the conditions under which acidobacterial *cbb* $_3$ -type TOs are employed for respiration. Our results extend the current knowledge on the respiratory flexibility of the prevalent *Acidobacteria*, which could help explain their success in the heterogeneous soil environment.

“Microaerobes” were previously defined as microorganisms that harbor high-affinity TOs in their genomes, either alone or in combination with low-affinity TOs, and use them to respire O_2 in microoxic environments (16). However, “microoxic” or subatmospheric concentrations of O_2 could be anything below 21% (vol/vol) O_2 , and within this range, the response of TOs can vary dramatically. In our study, we pushed microoxic to nanooxic conditions and explored the transcriptional response combined with enzyme kinetics to obtain a state-of-the-art assessment of their response to O_2 tension. We detected high- and low-affinity TOs in multiple acidobacterial genomes and respiration at nanomolar O_2 concentrations across the investigated strains. Yet our gene expression data did not indicate any detectable contribution of the *cbb* $_3$ -type high-affinity TOs at these O_2 concentrations; only one strain had contributions from the high-affinity *bd*-type TO. This suggests that the capability for microaerobic respiration in these acidobacteria is not solely due to the presence and associated activity of high-affinity TOs.

Instead, the acidobacterial microaerobic lifestyle seems to also be imparted by low-affinity *caa*₃-type TOs that enable them to respire O₂ at nanomolar concentrations. This illustrates that the presence of a high-affinity TO in a genome is not a prerequisite for microaerobic respiration. To that end, we would like to amend the definition of microaerobe to encompass microorganisms that are capable of respiring O₂ under microoxic conditions via the utilization of high- or low-affinity TOs. Furthermore, these findings demonstrate that it can be challenging to make predictions on the ecophysiology and lifestyle of microorganisms based solely on their genomic information, even for a process as well studied as aerobic respiration.

MATERIALS AND METHODS

Strains and growth conditions. Five chemoorganotrophic strains of the family *Acidobacteriaceae*, *Acidobacteriaceae* bacterium KBS 83 (DSM 24295), *Terriglobus* sp. TAA 43 (LMG 30954; DSM 24187), *Terriglobus roseus* KBS 63 (NRRL B-41598^T; DSM 18391), *Edaphobacter* sp. TAA 166 (LMG 30955; DSM 24188), and *Acidobacterium capsulatum* 161 (ATCC 51196; DSM 1124), were grown in vitamins and salts base (VSB) medium (51, 52) amended with 10 mM glucose as the sole carbon source at pH 6 or 5 (*A. capsulatum* 161). Additional information on the strains was reported previously (27, 52–54).

Setup and incubation for respiratory kinetic parameters. The details of the setup and experimental procedure were previously described (34, 42, 55). Briefly, the incubations were conducted in custom-made 500- or 1,100-ml glass bottles, which had been sequentially rinsed with a solution containing 0.1 M NaOH, 0.1 M HCl, and autoclaved water to prevent contamination. A continuous flow of N₂ was maintained while filling the bottles with N₂-purged medium and subsequent sealing with ground-glass stoppers. Exponential-phase acidobacterial cells were injected into these bottles (2 to 3 replicates/strain), while glass-coated magnetic stirrers homogenized the suspension. The O₂ concentration was optically determined every 20 s by luminescence-based O₂ sensors (Lumos) with sensor spots (measurement range, 0.5 to 1,500 nmol O₂ liter⁻¹) (56) glued onto the inside of the bottles. Bottles were incubated at room temperature and shielded from light for 24 h. Air-saturated water (4 to 5 ml) was repeatedly injected into the bottles after anoxia was reached by cell respiration, with peak concentrations ranging from 600 to 1,620 nmol O₂ liter⁻¹. One milliliter of the cell suspension was collected and fixed with 1% glutaraldehyde (Sigma-Aldrich, St. Louis, MO, USA) to determine cell numbers as described previously (42). After the incubations were completed, O₂ sensors were calibrated with oxygenated water and sodium dithionite.

Calculation of kinetic parameters. O₂ consumption rates were calculated from linear regression of O₂ concentrations over time in intervals of 6 min from the highest O₂ concentration down to anoxia. Kinetic parameters, the apparent half-saturation constant ($K_{m(\text{app})}$) and the maximum respiration rate (V_{max}) of the Michaelis-Menten equation, were estimated by performing nonlinear parametric fits on the respiration-versus-O₂-concentration curves for each replicate. V_{max} and $K_{m(\text{app})}$ were varied iteratively until the best fit was obtained by least-square fits using Solver in Microsoft Excel (57). Maximum respiration rates per cell (R_{max}) were calculated by dividing the population respiration rate (V_{max}) by cell numbers. Michaelis-Menten plots of respiration rates versus O₂ concentrations were obtained by fitting a Michaelis-Menten model to the data using the equation $V = (V_{\text{max}} \times [\text{O}_2]) / (K_m + [\text{O}_2])$, where V is the rate, V_{max} is the maximum rate (nanomoles of O₂ per liter per hour), K_m is the half-saturation constant (nanomoles of O₂ per liter), and $[\text{O}_2]$ is the substrate concentration (nanomoles of O₂ per liter). Additional modifications of the Michaelis-Menten equation and further corrections can be found in Text S1 (Supplemental Materials and Methods 1) and Tables S1 and S2 in the supplemental material.

Transcriptional profiling incubations. *Acidobacteriaceae* bacterium KBS 83, *T. roseus* KBS 63, and *A. capsulatum* 161 were grown in biological quadruplicates in glass bottles (Schott) containing 1 liter of VSB minimal medium amended with 10 mM glucose under fully aerated conditions. Once cells reached exponential phase, they were transferred into HCl-sterilized and autoclaved-water-rinsed glass bottles equipped with internally preglued sensing spots. Incubations were run for 225 min and split into four discrete, declining O₂ concentrations (10 μmol O₂ liter⁻¹, 1 μmol O₂ liter⁻¹, 0.1 μmol O₂ liter⁻¹, and 0.001 μmol O₂ liter⁻¹) down to anoxia (0 μmol O₂ liter⁻¹ is <0.0005 μmol O₂ liter⁻¹) obtained by purging with N₂-air mixtures (Table S3). O₂ concentrations were monitored by two Lumos systems with different sensitivity ranges (0.5 to 1,500 and 10 to 20,000 nmol O₂ liter⁻¹) (56). At every time point (Table S3), 30 to 50 ml of the culture was collected for RNA extractions by syringes prefilled with a phenol-stop solution (58). The sensor spots were calibrated after the incubations with oxygenated water and sodium dithionite. Additional details can be found in Text S1 (Supplemental Materials and Methods 2).

RNA extraction and purification. Total RNA was extracted from frozen cell pellets using an acidic phenol-chloroform-isoamyl alcohol protocol as described previously (59), with mechanical disruption (FastPrep-24 bead beater; MP Biomedicals, Heidelberg, Germany). The extraction supernatant was purified using standard chloroform-isoamyl alcohol purification, and RNA was precipitated using a polyethylene glycol (PEG) solution and RNA-grade glycogen by centrifugation (21,130 × *g* for 1 h at 4°C). Coextracted DNA was digested using a Turbo DNA-free kit (Thermo Fisher), and complete DNA removal was verified by failure to obtain quantitative PCR (qPCR) amplification products with the purified RNA template, targeting the *rpoB* gene encoding the β subunit of the DNA-directed RNA polymerase, under the qPCR conditions described in Table S4. A more detailed protocol can be found in Text S1 (Supplemental Materials and Methods 3).

Primer design, cDNA synthesis, RT-qPCR, and data analysis. Specifications of the newly designed primers targeting the catalytic subunits (subunit I) of the TOs are listed in Table S4. See Text S1 (Supplemental Materials and Methods 4) for details on primer design, cDNA synthesis, reverse transcription-qPCR (RT-qPCR), and data analysis.

Transcriptome sequencing. Triplicate total RNA samples of *Acidobacteriaceae* bacterium KBS 83, *T. roseus* KBS 63, and *A. capsulatum* 161 from selected O₂ concentrations and time points were sent to the Vienna BioCenter Core Facilities. rRNA was depleted using the New England Biolabs (NEB) Ribo-Zero rRNA removal kit for bacteria. Sequencing was performed on an Illumina NextSeq 550 system, resulting in a total of 36 samples with 8.2 million to 18.2 million 75-nucleotide reads each.

Transcriptome data processing and statistical analyses. Raw reads were trimmed of sequencing adapters and low-quality 3' ends using BBduk (BBtools v37.61; <https://jgi.doe.gov/data-and-tools/bbtools/>) with default parameters and error corrected using the Bayes-Hammer module of SPAdes assembler version 3.13.0 (60). Any reads mapping to either SILVA small-subunit (SSU) or large-subunit (LSU) release 132 (61) or the 5S rRNA database (62) with a sequence identity of >70% (performed with BBmap and BBtools; <https://jgi.doe.gov/data-and-tools/bbtools/>) were removed from the data set. The remaining reads were mapped to the publicly available genomes of the acidobacterial strains (53). The RNA reads per gene were summarized using the featureCounts tool from the Subread package v1.6.2 (63). Based on the generated read count tables, transcripts per million were calculated in R v3.6.0. Differential expression analyses, such as calculations of log₂ fold changes of relative transcript abundances and the significance of these changes, were performed in DESeq2 v1.26.0 using default parameters and a *P* value cutoff of 0.05 (64).

Data availability. The raw transcriptomic reads are available under BioProject accession number PRJNA635786. The code and pipelines used for data analysis are available upon request.

SUPPLEMENTAL MATERIAL

Supplemental material is available online only.

TEXT S1, DOCX file, 0.04 MB.

FIG S1, EPS file, 1.1 MB.

TABLE S1, DOCX file, 0.01 MB.

TABLE S2, DOCX file, 0.02 MB.

TABLE S3, DOCX file, 0.01 MB.

TABLE S4, DOCX file, 0.02 MB.

TABLE S5, DOCX file, 0.02 MB.

DATA SET S1, XLSX file, 0.02 MB.

DATA SET S2, XLSX file, 0.03 MB.

ACKNOWLEDGMENTS

We thank the Division of Computational Systems Biology for providing and maintaining the Life Science Compute Cluster (LiSC) at the University of Vienna. We are grateful to Lars B. Pedersen at Aarhus University for his technical assistance and to Sergey Borisov at the Technical University of Graz for the production of optical oxygen sensors.

This work was funded by an Austrian Science Fund (FWF) project grant (grant number P26392-B20 to D.W. and S.A.E.), an ERDF Operational Programme and the Regional Government of Andalusia (project reference FEDER-UCA18-107225 to E.G.-R.), and the Dr. Anton Oelzelt-Newin'sche Stiftung of the Austrian Academy of Sciences (ÖAW). Support for the kinetic measurements and flow cytometry counts was obtained from the Poul Due Jensen Foundation.

REFERENCES

- Jarecke KM, Loecke TD, Burgin AJ. 2016. Coupled soil oxygen and greenhouse gas dynamics under variable hydrology. *Soil Biol Biochem* 95:164–172. <https://doi.org/10.1016/j.soilbio.2015.12.018>.
- Hosler JP, Ferguson-Miller S, Mills DA. 2006. Energy transduction: proton transfer through the respiratory complexes. *Annu Rev Biochem* 75:165–187. <https://doi.org/10.1146/annurev.biochem.75.062003.101730>.
- Richter OMH, Ludwig B. 2009. Electron transfer and energy transduction in the terminal part of the respiratory chain—lessons from bacterial model systems. *Biochim Biophys Acta* 1787:626–634. <https://doi.org/10.1016/j.bbabi.2009.02.020>.
- Sousa FL, Alves RJ, Ribeiro M, Pereira-Leal JB, Teixeira M, Pereira MM. 2012. The superfamily of heme-copper oxygen reductases: types and evolutionary considerations. *Biochim Biophys Acta* 1817:629–637. <https://doi.org/10.1016/j.bbabi.2011.09.020>.
- Rice CW, Hempfling WP. 1978. Oxygen-limited continuous culture and respiratory energy conservation in *Escherichia coli*. *J Bacteriol* 134:115–124. <https://doi.org/10.1128/jb.134.1.115-124.1978>.
- Arslan E, Kannt A, Thöny-Meyer L, Hennecke H. 2000. The symbiotically essential *cbb*₃-type oxidase of *Bradyrhizobium japonicum* is a proton pump. *FEBS Lett* 470:7–10. [https://doi.org/10.1016/S0014-5793\(00\)01277-1](https://doi.org/10.1016/S0014-5793(00)01277-1).
- Preisig O, Zufferey R, Thöny-Meyer L, Appleby C, Hennecke H. 1996. A high-affinity *cbb*₃-type cytochrome oxidase terminates the symbiosis-specific respiratory chain of *Bradyrhizobium japonicum*. *J Bacteriol* 178:1532–1538. <https://doi.org/10.1128/jb.178.6.1532-1538.1996>.

8. Arai H, Kawakami T, Osamura T, Hirai T, Sakai Y, Ishii M. 2014. Enzymatic characterization and *in vivo* function of five terminal oxidases in *Pseudomonas aeruginosa*. *J Bacteriol* 196:4206–4215. <https://doi.org/10.1128/JB.02176-14>.
9. Jackson RJ, Elvers KT, Lee LJ, Gidley MD, Wainwright LM, Lightfoot J, Park SF, Poole RK. 2007. Oxygen reactivity of both respiratory oxidases in *Campylobacter jejuni*: the *cydAB* genes encode a cyanide-resistant, low-affinity oxidase that is not of the cytochrome *bd* type. *J Bacteriol* 189:1604–1615. <https://doi.org/10.1128/JB.00897-06>.
10. Borisov VB. 1996. Cytochrome *bd*: structure and properties. *Biokhimiia* 61:786–799.
11. Borisov VB, Gennis RB, Hemp J, Verkhovskiy MI. 2011. The cytochrome *bd* respiratory oxygen reductases. *Biochim Biophys Acta* 1807:1398–1413. <https://doi.org/10.1016/j.bbabi.2011.06.016>.
12. Safarian S, Rajendran C, Müller H, Preu J, Langer JD, Ovcinnikov S, Hirose T, Kusumoto T, Sakamoto J, Michel H. 2016. Structure of a *bd* oxidase indicates similar mechanisms for membrane integrated oxygen reductases. *Science* 352:583–586. <https://doi.org/10.1126/science.aaf2477>.
13. D'mello R, Hill S, Poole RK. 1996. The cytochrome *bd* quinol oxidase in *Escherichia coli* has an extremely high oxygen affinity and two oxygen-binding haems: implications for regulation of activity *in vivo* by oxygen inhibition. *Microbiology (Reading)* 142:755–763. <https://doi.org/10.1099/00221287-142-4-755>.
14. Poole RK, Cook GM. 2000. Redundancy of aerobic respiratory chains in bacteria? Routes, reasons and regulation. *Adv Microb Physiol* 43:165–224. [https://doi.org/10.1016/s0065-2911\(00\)43005-5](https://doi.org/10.1016/s0065-2911(00)43005-5).
15. Bueno E, Mesa S, Bedmar EJ, Richardson DJ, Delgado MJ. 2012. Bacterial adaptation of respiration from oxic to microoxic and anoxic conditions: redox control. *Antioxid Redox Signal* 16:819–852. <https://doi.org/10.1089/ars.2011.4051>.
16. Morris RL, Schmidt TM. 2013. Shallow breathing: bacterial life at low O₂. *Nat Rev Microbiol* 11:205–212. <https://doi.org/10.1038/nrmicro2970>.
17. Pasteur L. 1876. Études sur la bière: ses maladies, causes qui les Provoquent, procédé pour la rendre inaltérable; avec une theorie nouvelle de la fermentation. Gauthier-Villars, Paris, France.
18. Stolper DA, Revsbech NP, Canfield DE. 2010. Aerobic growth at nanomolar oxygen concentrations. *Proc Natl Acad Sci U S A* 107:18755–18760. <https://doi.org/10.1073/pnas.1013435107>.
19. Gong X, Garcia-Robledo E, Lund MB, Lehner P, Borisov SM, Klimant I, Revsbech NP, Schramm A. 2018. Gene expression of terminal oxidases in two marine bacterial strains exposed to nanomolar oxygen concentrations. *FEMS Microbiol Ecol* 94:fy072. <https://doi.org/10.1093/femsec/fy072>.
20. Liptzin D, Silver WL, Detto M. 2011. Temporal dynamics in soil oxygen and greenhouse gases in two humid tropical forests. *Ecosystems* 14:171–182. <https://doi.org/10.1007/s10021-010-9402-x>.
21. Silver WL, Lugo AE, Keller M. 1999. Soil oxygen availability and biogeochemistry along rainfall and topographic gradients in upland wet tropical forest soils. *Biogeochemistry* 44:301–328. <https://doi.org/10.1007/BF00996995>.
22. Delgado-Baquero M, Oliverio AM, Brewer TE, Benavent-González A, Eldridge DJ, Bardgett RJ, Maestre FT, Singh BK, Fierer N. 2018. A global atlas of the dominant bacteria found in soil. *Science* 359:320–325. <https://doi.org/10.1126/science.aap9516>.
23. Dedysh SN, Yilmaz P. 2018. Refining the taxonomic structure of the phylum *Acidobacteria*. *Int J Syst Evol Microbiol* 68:3796–3806. <https://doi.org/10.1099/ijsem.0.003062>.
24. Kielak AM, Barreto CC, Kowalchuk GA, van Veen JA, Kuramae EE. 2016. The ecology of *Acidobacteria*: moving beyond genes and genomes. *Front Microbiol* 7:744. <https://doi.org/10.3389/fmicb.2016.00744>.
25. Crowther TW, van den Hoogen J, Wan J, Mayes MA, Keiser AD, Mo L, Averill C, Maynard DS. 2019. The global soil community and its influence on biogeochemistry. *Science* 365:eaav0550. <https://doi.org/10.1126/science.aav0550>.
26. Fierer N. 2017. Embracing the unknown: disentangling the complexities of the soil microbiome. *Nat Rev Microbiol* 15:579–590. <https://doi.org/10.1038/nrmicro.2017.87>.
27. Eichorst SA, Trojan D, Roux S, Herbold C, Rattei T, Woebken D. 2018. Genomic insights into the *Acidobacteria* reveal strategies for their success in terrestrial environments. *Environ Microbiol* 20:1041–1063. <https://doi.org/10.1111/1462-2920.14043>.
28. Tecon R, Or D. 2017. Biophysical processes supporting the diversity of microbial life in soil. *FEMS Microbiol Rev* 41:599–623. <https://doi.org/10.1093/femsre/fux039>.
29. Sexstone AJ, Revsbech NP, Parkin TB, Tiedje JM. 1985. Direct measurement of oxygen profiles and denitrification rates in soil aggregates. *Soil Sci Soc Am J* 49:645–651. <https://doi.org/10.2136/sssaj1985.03615995004900030024x>.
30. Borer B, Tecon R, Or D. 2018. Spatial organization of bacterial populations in response to oxygen and carbon counter-gradients in pore networks. *Nat Commun* 9:769. <https://doi.org/10.1038/s41467-018-03187-y>.
31. Brune A, Frenzel P, Cypionka H. 2000. Life at the oxic-anoxic interface: microbial activities and adaptations. *FEMS Microbiol Rev* 24:691–710. <https://doi.org/10.1111/j.1574-6976.2000.tb00567.x>.
32. Bristow LA, Dalsgaard T, Tiano L, Mills DB, Bertagnolli AD, Wright JJ, Hallam SJ, Ulloa O, Canfield DE, Revsbech NP, Thamdrup B. 2016. Ammonium and nitrite oxidation at nanomolar oxygen concentrations in oxygen minimum zone waters. *Proc Natl Acad Sci U S A* 113:10601–10606. <https://doi.org/10.1073/pnas.1600359113>.
33. Kalvelage T, Lavik G, Jensen MM, Revsbech NP, Löscher C, Schunck H, Desai DK, Hauss H, Kiko R, Holtappels M, Laroche J, Schmitz RA, Graco MI, Kuypers MMM. 2015. Aerobic microbial respiration in oceanic oxygen minimum zones. *PLoS One* 10:e0133526. <https://doi.org/10.1371/journal.pone.0133526>.
34. Garcia-Robledo E, Padilla CC, Aldunate M, Stewart FJ, Ulloa O, Paulmier A, Gregori G, Revsbech NP. 2017. Cryptic oxygen cycling in anoxic marine zones. *Proc Natl Acad Sci U S A* 114:8319–8324. <https://doi.org/10.1073/pnas.1619844114>.
35. Refojo PN, Sousa FL, Teixeira M, Pereira MM. 2010. The alternative complex III: a different architecture using known building modules. *Biochim Biophys Acta* 1797:1869–1876. <https://doi.org/10.1016/j.bbabi.2010.04.012>.
36. Hausmann B, Pelikan C, Herbold CW, Köstlbacher S, Albertsen M, Eichorst SA, Glavina Del Rio T, Huemer M, Nielsen PH, Rattei T, Stingl U, Tringe SG, Trojan D, Wentrup C, Woebken D, Pester M, Loy A. 2018. Peatland *Acidobacteria* with a dissimilatory sulfur metabolism. *ISME J* 12:1729–1742. <https://doi.org/10.1038/s41396-018-0077-1>.
37. Sun C, Benlekbir S, Venkatakrisnan P, Wang Y, Hong S, Hosler J, Tajkhorshid E, Rubinstein JL, Gennis RB. 2018. Structure of the alternative complex III in a supercomplex with cytochrome oxidase. *Nature* 557:123–126. <https://doi.org/10.1038/s41586-018-0061-y>.
38. Wiseman B, Nitharwal RG, Fedotovskaya O, Schäfer J, Guo H, Kuang Q, Benlekbir S, Sjöstrand D, Ädelroth P, Rubinstein JL, Brzezinski P, Högbom M. 2018. Structure of a functional obligate complex III/IIV2 respiratory supercomplex from *Mycobacterium smegmatis*. *Nat Struct Mol Biol* 25:1128–1136. <https://doi.org/10.1038/s41594-018-0160-3>.
39. Sousa JS, Calisto F, Langer JD, Mills DJ, Refojo PN, Teixeira M, Kühlbrandt W, Vonck J, Pereira MM. 2018. Structural basis for energy transduction by respiratory alternative complex III. *Nat Commun* 9:1728. <https://doi.org/10.1038/s41467-018-04141-8>.
40. Letts JA, Sazanov LA. 2017. Clarifying the supercomplex: the higher-order organization of the mitochondrial electron transport chain. *Nat Struct Mol Biol* 24:800–808. <https://doi.org/10.1038/nsmb.3460>.
41. Ducluzeau A-L, Ouchane S, Nitschke W. 2008. The *ccb₃* oxidases are an ancient innovation of the domain bacteria. *Mol Biol Evol* 25:1158–1166. <https://doi.org/10.1093/molbev/msn062>.
42. Gong X, Garcia-Robledo E, Schramm A, Revsbech NP. 2016. Respiratory kinetics of marine bacteria exposed to decreasing oxygen concentrations. *Appl Environ Microbiol* 82:1412–1422. <https://doi.org/10.1128/AEM.03669-15>.
43. Markföged R, Nielsen LP, Nyord T, Ottosen LDM, Revsbech NP. 2011. Transient N₂O accumulation and emission caused by O₂ depletion in soil after liquid manure injection. *Eur J Soil Sci* 62:541–550. <https://doi.org/10.1111/j.1365-2389.2010.01345.x>.
44. Rauhamäki V, Wikström M. 2014. The causes of reduced proton-pumping efficiency in type B and C respiratory heme-copper oxidases, and in some mutated variants of type A. *Biochim Biophys Acta* 1837:999–1003. <https://doi.org/10.1016/j.bbabi.2014.02.020>.
45. Wikström M, Sharma V, Kaila VRI, Hosler JP, Hummer G. 2015. New perspectives on proton pumping in cellular respiration. *Chem Rev* 115:2196–2221. <https://doi.org/10.1021/cr500448t>.
46. Le Laz S, Kpebe A, Bauzan M, Lignon S, Rousset M, Brugna M. 2016. Expression of terminal oxidases under nutrient-starved conditions in *Shewanella oneidensis*: detection of the A-type cytochrome c oxidase. *Sci Rep* 6:19726. <https://doi.org/10.1038/srep19726>.
47. Giuffrè A, Borisov VB, Arese M, Sarti P, Forte E. 2014. Cytochrome *bd* oxidase and bacterial tolerance to oxidative and nitrosative stress. *Biochim Biophys Acta* 1837:1178–1187. <https://doi.org/10.1016/j.bbabi.2014.01.016>.

48. Buschmann S, Warkentin E, Xie H, Langer JD, Ermler U, Michel H. 2010. The structure of *cbb*₃ cytochrome oxidase provides insights into proton pumping. *Science* 329:327–330. <https://doi.org/10.1126/science.1187303>.
49. Lamrabet O, Pieulle L, Aubert C, Mouhamar F, Stocker P, Dolla A, Brasseur G. 2011. Oxygen reduction in the strict anaerobe *Desulfovibrio vulgaris* Hildenborough: characterization of two membrane-bound oxygen reductases. *Microbiology (Reading)* 157:2720–2732. <https://doi.org/10.1099/mic.0.049171-0>.
50. D'Mello R, Hill S, Poole RK. 1994. Determination of the oxygen affinities of terminal oxidases in *Azotobacter vinelandii* using the deoxygenation of oxyleghaemoglobin and oxymyoglobin: cytochrome *bd* is a low-affinity oxidase. *Microbiology (Reading)* 140:1395–1402. <https://doi.org/10.1099/00221287-140-6-1395>.
51. Stevenson BS, Eichorst SA, Wertz JT, Schmidt TM, Breznak JA. 2004. New strategies for cultivation and detection of previously uncultured microbes. *Appl Environ Microbiol* 70:4748–4755. <https://doi.org/10.1128/AEM.70.8.4748-4755.2004>.
52. Eichorst SA, Breznak JA, Schmidt TM. 2007. Isolation and characterization of soil bacteria that define *Terriglobus* gen. nov., in the phylum *Acidobacteria*. *Appl Environ Microbiol* 73:2708–2717. <https://doi.org/10.1128/AEM.02140-06>.
53. Eichorst SA, Trojan D, Huntemann M, Clum A, Pillay M, Palaniappan K, Varghese N, Mikhailova N, Stamatis D, Reddy TBK, Daum C, Goodwin LA, Shapiro N, Ivanova N, Kyrpides N, Woyke T, Woebken D. 2020. One complete and seven draft genome sequences of subdivision 1 and 3 *Acidobacteria* isolated from soil. *Microbiol Resour Announc* 9:e01087-19. <https://doi.org/10.1128/MRA.01087-19>.
54. Eichorst SA, Kuske CR, Schmidt TM. 2011. Influence of plant polymers on the distribution and cultivation of bacteria in the phylum *Acidobacteria*. *Appl Environ Microbiol* 77:586–596. <https://doi.org/10.1128/AEM.01080-10>.
55. Tiano L, Garcia-Robledo E, Revsbech NP. 2014. A new highly sensitive method to assess respiration rates and kinetics of natural planktonic communities by use of the switchable trace oxygen sensor and reduced oxygen concentrations. *PLoS One* 9:e105399. <https://doi.org/10.1371/journal.pone.0105399>.
56. Lehner P, Larndorfer C, Garcia-Robledo E, Larsen M, Borisov SM, Revsbech NP, Glud RN, Canfield DE, Klimant I. 2015. LUMOS—a sensitive and reliable optode system for measuring dissolved oxygen in the nanomolar range. *PLoS One* 10:e0128125. <https://doi.org/10.1371/journal.pone.0128125>.
57. Kemmer G, Keller S. 2010. Nonlinear least-squares data fitting in Excel spreadsheets. *Nat Protoc* 5:267–281. <https://doi.org/10.1038/nprot.2009.182>.
58. Kits KD, Klotz MG, Stein LY. 2015. Methane oxidation coupled to nitrate reduction under hypoxia by the gammaproteobacterium *Methylomonas denitrificans*, sp. nov. type strain FJG1. *Environ Microbiol* 17:3219–3232. <https://doi.org/10.1111/1462-2920.12772>.
59. Angel R. 2012. Total nucleic acid extraction from soil. *Protoc Exch* <https://doi.org/10.1038/protex.2012.046>.
60. Nikolenko SI, Korobeynikov AI, Alekseyev MA. 2013. BayesHammer: Bayesian clustering for error correction in single-cell sequencing. *BMC Genomics* 14:S7. <https://doi.org/10.1186/1471-2164-14-S1-S7>.
61. Quast C, Pruesse E, Yilmaz P, Gerken J, Schweer T, Yarza P, Peplies J, Glockner FO. 2013. The SILVA ribosomal RNA gene database project: improved data processing and Web-based tools. *Nucleic Acids Res* 41: D590–D596. <https://doi.org/10.1093/nar/gks1219>.
62. Szymanski M, Zielezinski A, Barciszewski J, Erdmann VA, Karlowski WM. 2016. 5SRNadb: an information resource for 5S ribosomal RNAs. *Nucleic Acids Res* 44:D180–D183. <https://doi.org/10.1093/nar/gkv1081>.
63. Liao Y, Smyth GK, Shi W. 2014. FeatureCounts: an efficient general purpose program for assigning sequence reads to genomic features. *Bioinformatics* 30:923–930. <https://doi.org/10.1093/bioinformatics/btt656>.
64. Love MI, Huber W, Anders S. 2014. Moderated estimation of fold change and dispersion for RNA-seq data with DESeq2. *Genome Biol* 15:550. <https://doi.org/10.1186/s13059-014-0550-8>.